

OBSERVABILITY FOR NONLINEAR SYSTEMS: CONNECTING VARIATIONAL DYNAMICS, LYAPUNOV EXPONENTS, AND EMPIRICAL GRAMIANS

Mohamad H. Kazma, *Graduate Student Member, IEEE* and Ahmad F. Taha[◊], *Member, IEEE*

Abstract—Observability quantification is a key problem in dynamic network sciences. While it has been thoroughly studied for linear systems, observability quantification for nonlinear networks is less intuitive and more cumbersome. One common approach to quantify observability for nonlinear systems is via the *Empirical Gramian* (Empr-Gram)—a generalized form of the Gramian of linear systems. In this paper, we produce three new results. First, we establish that a variational form of discrete-time autonomous nonlinear systems (computed via perturbing initial conditions) yields a so-called *Variational Gramian* (Var-Gram) that is equivalent to the classic Empr-Gram; the former being easier to compute than the latter. Via *Lyapunov exponents* derived from Lyapunov’s direct method, the paper’s second result derives connections between existing observability measures and Var-Gram. The third result demonstrates the applicability of these new notions for sensor selection/placement in nonlinear systems. Numerical case studies demonstrate these three developments and their merits.

Index Terms—Nonlinear variational dynamics, nonlinear observability, observability Gramian, Lyapunov exponents.

I. INTRODUCTION AND CONTRIBUTIONS

Observability is most generally defined as the ability to reconstruct the states of a dynamic system from limited output measurements [1]. For linear systems, quantifying observability is well-established [2]. However, the direct extension of observability notions from linear systems to nonlinear systems is not straightforward. We briefly discuss this literature next.

A differential approach introduced in [3] evaluates observability by computing the *Lie derivatives* around an initial point. Lie derivatives are typically avoided in practice for two reasons. (i) Lie derivatives are computationally expensive and require the calculation of higher order derivatives [4], and (ii) the resulting observability measure is a rank condition that is qualitative in nature [5] and difficult to optimize. That is, the quantification is binary and thus does not lend it self easily to optimization problems such as sensor selection.

Other formulations can also be utilized to assess a nonlinear system’s observability. One method follows from formulating the *empirical observability Gramian* (Empr-Gram) of the system by considering an impulse response approach [6]–[9]. It is noted that scaling the internal states and output measurements

so that the Gramian’s eigenvalues capture the local variations in states is not straightforward [5]. Furthermore, the Empr-Gram can be extended to account for stochastic nonlinear systems from a statistical point of view, as proposed in [9]. A moving horizon approach for discretized nonlinear dynamics is introduced in [10] and further developed in [11]; it is based on a moving horizon formulation and offers a more robust solution than the Empr-Gram. The proposed approach does not establish a direct relation to the linear observability Gramian and the notions of Lyapunov stability.

Lyapunov’s second method is considered as a basis for observability of linear systems, yet a general theory to formulate Lyapunov functions for nonlinear systems is lacking [12]. In the fields of chaos and ergodicity, a well-known method for assessing the stability of nonlinear system trajectory stems from Lyapunov’s direct method on stability [13]. The direct method provides a characteristic spectrum of *Lyapunov exponents* that yields a basis for exponential asymptotic stability of dynamical systems. This often-overlooked notion of stability in the field of control theory has recently been investigated in several areas. This includes studies that are related to bounds and observer design for linear time-varying systems [14] and model predictive control [15].

An important aspect of the aforementioned stability method is that it is based on a *variational* representation of the dynamical system [16], which means that the system is represented by the evolution of infinitesimal state variations along its trajectory. Such variational system representations are considered for a wide class of nonlinear systems [17]. The variational system can be viewed as a linear time-varying model constructed along the tangent space of the nonlinear system [18], rendering the computation of an observability Gramian more efficient. In a recent study, considering a variational system representation of the general state-space formulation introduced in [17], an *empirical differential Gramian* is formulated for the continuous-time domain [18]. The introduced Gramian is similar to the Empr-Gram [6], [8]; both are based on impulse response and empirical data, rendering both formulations computationally intensive. The impulse response around an initial state results in a fixed state trajectory. As such, for nonlinear systems the aforementioned observability results are considered local state trajectory dependent.

In this paper, we introduce a nonlinear observability Gramian that is based on a discrete-time variational representation. Our first objective is to illustrate that the proposed *variational observability Gramian* (Var-Gram) is equivalent to Empr-Gram; the former being more computationally efficient.

[◊]Corresponding author. This work is supported by National Science Foundation under Grants 2152450 and 2151571. The authors are with the Civil & Environmental Engineering and Electrical & Computer Engineering Departments, Vanderbilt University, 2201 West End Ave, Nashville, Tennessee 37235. Emails: mohamad.h.kazma@vanderbilt.edu, ahmad.taha@vanderbilt.edu.

We also show that the Var-Gram reduces to the linear Gramian for a time-invariant linear system. The second objective is to illustrate the connections relating Lyapunov exponents and Var-Gram measures. Then based on the proposed Var-Gram, we introduce conditions for observability of general nonlinear systems. The third objective is to showcase how these aforementioned developments can be applied to solve the sensor node selection (SNS) problem efficiently for nonlinear systems, which heavily relies on quantifying observability.

Paper Contributions. The main contributions of this paper are three-fold. (i) We formulate a new method for computing the observability Gramian of nonlinear systems with no inputs. This method is derived from a variational system representation of discrete-time nonlinear dynamics. We show and provide evidence that the proposed Var-Gram is equivalent to the Empr-Gram; it reduces to the linear Gramian for a stable linear time-invariant (LTI) system. (ii) We show that observability measures under Var-Gram are equivalent to Lyapunov exponents. We derive a local observability condition for nonlinear systems that is based on the spectral radius of the proposed Gramian. Such condition offers a bound for the observability of the systems in relation to Lyapunov exponents. (iii) We show that the Var-Gram is a modular set function under sensor allocation parameterization vector and that specific observability measures based on the proposed Var-Gram are submodular. This submodularity enables the solution of the SNS problem in nonlinear networks to be scalable. This is analogous to SNS in linear networks where the submodularity of the linear Gramian is well-established.

Broader Impacts. Establishing the connection between nonlinear observability and the Lyapunov spectrum of exponents allows us to leverage the plethora of data-driven methods for computing Lyapunov exponents; see [19] and references therein. Based on such methods, nonlinear observability can be evaluated from a data-driven perspective. Furthermore, the established relations between Lyapunov exponents and dynamical properties, such as entropy [20], allow for studying observability in stochastic and chaotic dynamical systems. Investigating the above prospects is outside the scope of this paper.

Paper Organization. The paper is organized as follows: Section II introduces the problem formulation and provides preliminaries on nonlinear observability. In Section III we develop the theory behind the construction of the proposed observability Gramian. The connection between the Var-Gram and Lyapunov exponents is presented in Section IV. Section V presents the Var-Gram properties for the SNS problem in nonlinear systems. The numerical results and the SNS problem are presented in Section VI. Section VII concludes this paper.

Notation. Let \mathbb{N} , \mathbb{R} , \mathbb{R}^n , and $\mathbb{R}^{p \times q}$ denote the set of natural numbers, real numbers, real-valued row vectors with size of n , and p -by- q real matrices respectively. The symbol \otimes denotes the Kronecker product. The cardinality of a set \mathcal{N} is denoted by $|\mathcal{N}|$. The operators $\det(\mathbf{A})$, $\text{rank}(\mathbf{A})$ and $\text{trace}(\mathbf{A})$ return the determinant, rank and trace of matrix \mathbf{A} . The operator $\{\mathbf{x}_i\}_{i=0}^N \in \mathbb{R}^{Nn}$ constructs a column vector that concatenates vectors $\mathbf{x}_i \in \mathbb{R}^n$ for all $i \in \{0, 1, \dots, N\}$. The dot-product of two matrix-valued vectors $\boldsymbol{\xi}$ is represented as $\langle \boldsymbol{\xi}, \boldsymbol{\xi} \rangle := \boldsymbol{\xi}^\top \boldsymbol{\xi}$,

where the superscript \top denotes the transpose. The \mathcal{L}_2 -norm of vector \mathbf{x} is denoted by $\|\mathbf{x}\|_2 := \sqrt{\langle \mathbf{x}, \mathbf{x} \rangle}$. For a matrix \mathbf{A} , $\|\mathbf{A}\|_2$ denotes the induced \mathcal{L}_2 -norm. The operator $\mathbf{h} \circ \mathbf{f} := \mathbf{h}(\mathbf{f}(\mathbf{x}))$ denotes the composition of functions. The notation t_0 and t (as subscripts and superscripts) of a flow mapping are used for continuous-time mappings, while 0 and k are used for discrete-time mappings.

II. PRELIMINARIES AND DEFINITIONS

Let the following represent a general continuous-time nonlinear dynamic network without input.

$$\dot{\mathbf{x}}(t) = \mathbf{f}(\mathbf{x}(t)), \quad \mathbf{y}(t) = \mathbf{h}(\mathbf{x}(t)), \quad (1)$$

where the smooth manifold $\mathcal{M} \subseteq \mathbb{R}^{n_x}$ represents the state-space under the action of system dynamics, the system state vector evolving in \mathcal{M} is denoted as $\mathbf{x}(t) := \mathbf{x} \in \mathbb{R}^{n_x}$, and $\mathbf{y}(t) := \mathbf{y} \in \mathbb{R}^{n_y}$ is the global output measurement vector. The nonlinear mapping function $\mathbf{f}(\cdot) : \mathcal{M} \rightarrow \mathbb{R}^{n_x}$ and nonlinear mapping measurement function $\mathbf{h}(\cdot) : \mathcal{M} \rightarrow \mathbb{R}^{n_y}$ are smooth and at least twice continuously differentiable.

Assumption II.1: For any system initialization at $\mathbf{x}_0 \in \mathcal{X}_0$, the system remains in $\mathcal{X} \subseteq \mathcal{M}$ for any $t \geq 0$, such that the compact set \mathcal{X} contains the set of feasible solutions of the system.

This assumption dictates that \mathbf{x} belongs to a compact set \mathcal{X} along the system trajectory. This is not restrictive when considering nonlinear networks such as cyber-physical networks with bounded states.

In this manuscript, we consider a discrete-time nonlinear dynamical system without inputs, representing the action of the system dynamics evolving on the smooth manifold \mathcal{M} . The proposed methods and SNS framework are developed while considering discrete-time models. We introduce the continuous model (1) to establish nonlinear observability concepts in Section II-A and to derive Proposition III.1. The numerical discretization of the continuous-time model renders a system amenable towards various control applications. In this paper, the *implicit Runge-Kutta* (IRK) method [21] is the discretization method of choice. There are a myriad of discretization methods for general nonlinear systems—refer to [22]. The IRK method is utilized since it offers a wide-range of application to systems with various degrees of stiffness. The following form represents the continuous-time nonlinear system (1) rewritten in a discrete-time representation

$$\mathbf{x}_{k+1} = \mathbf{x}_k + \tilde{\mathbf{f}}(\mathbf{x}_k), \quad (2a)$$

$$\mathbf{y}_k = \mathbf{h}(\mathbf{x}_k), \quad (2b)$$

where $k \in \mathbb{N}$ is the discrete-time index such that $\mathbf{x}_k = \mathbf{x}(kT)$ and $T > 0$ denote the discretization period. The nonlinear mapping function $\tilde{\mathbf{f}}(\cdot) \in \mathbb{R}^{n_x}$ represents the dynamics depicted by $\mathbf{f}(\cdot)$ under the action of a discrete-time model. The nonlinear mapping function $\tilde{\mathbf{f}}(\cdot)$ is defined for the IRK method as $\tilde{\mathbf{f}}(\mathbf{x}_k) := \frac{T}{4}(\mathbf{f}(\boldsymbol{\zeta}_{1,k+1}) + 3\mathbf{f}(\boldsymbol{\zeta}_{2,k+1}))$. Vectors $\boldsymbol{\zeta}_{1,k+1}, \boldsymbol{\zeta}_{2,k+1} \in \mathbb{R}^{n_x}$ are auxiliary for computing \mathbf{x}_{k+1} provided that \mathbf{x}_k is given. Refer to Appendix A for additional information regarding the IRK discretization method's auxiliary vectors.

A. Observability of Nonlinear Systems

To make this paper self-contained, we briefly recall the notions of nonlinear observability. Consider $\phi_{t_0}^t : \mathcal{M} \rightarrow \mathcal{M}$ which maps a state $\mathbf{x}_0 \in \mathcal{X}_0$ at initial time t_0 to a state $\mathbf{x} \in \mathcal{X}$ at time $t > 0$ [21], [23]. The continuous-time flow map of nonlinear system (1) can be written as

$$\phi_{t_0}^t(\mathbf{x}_0) := \mathbf{x}(t) = \mathbf{x}(t_0) + \int_{t_0}^t \mathbf{f}(\mathbf{x}(\tau)) d\tau. \quad (3)$$

This interpretation of the nonlinear dynamical system (1) defines the flow of phase points along the phase curve, thereby describing the time evolution of the states pertaining to the dynamical system [24]. The composition mapping of (3) under the action of the measurement equation can be denoted as $\mathbf{h} \circ \phi_{t_0}^t(\mathbf{x}_0)$ for $t \in [t_0, t]$. Observability of the nonlinear dynamical system is then defined as the ability to identify the initial states \mathbf{x}_0 satisfying Assumption II.1 for $t > t_0$. Definitions II.1 and II.2 are based on the notions of observability from the work of Hermann and Krener [3].

Definition II.1 (distinguishability [3]): Any two points \mathbf{x}_1 and $\mathbf{x}_2 \in \mathcal{X}_0$ are *indistinguishable* if and only if for any $\phi_{t_0}^t \in \mathcal{X}$, we have $\mathbf{h} \circ \phi_{t_0}^t(\mathbf{x}_1) = \mathbf{h} \circ \phi_{t_0}^t(\mathbf{x}_2)$.

Definition II.2 (local observability [3]): A nonlinear system is *locally weakly observable* at \mathbf{x}_0 if there exists a neighborhood $\mathcal{D} \in \mathcal{X}_0$ such that $\mathbf{h} \circ \phi_{t_0}^t(\mathbf{x}_0) \neq \mathbf{h} \circ \phi_{t_0}^t(\mathbf{x}_1)$ for $t > t_0$ for all $\mathbf{x}_0 \neq \mathbf{x}_1 \in \mathcal{D}$, i.e., if the compositions are distinguishable. It is *locally observable* if for all $\mathbf{x}_0 \in \mathcal{X}_0$ it is *locally weakly observable*.

A seemingly stronger definition of observability (Definition II.2) for continuous systems is investigated in [25]. It shows that an observation window of finite length $N > 0$ exists given the realization of distinguishability (Definition II.1). Such sequence of measurements uniquely determines the initial state \mathbf{x}_0 on the compact set \mathcal{X}_0 . The existence of such finite-observation window defines the *uniform observability* criterion for discrete-time nonlinear systems [26].

Definition II.3 (uniform observability [26]): The system (2) is said to be *uniformly observable* over compact set \mathcal{X} if there exists a finite observability window $N > 0$ such that the output sequence

$$\xi(\mathbf{x}_0) := \{\mathbf{y}_i\}_{i=0}^{N-1} \in \mathbb{R}^{Nn_y}, \quad (4)$$

is injective (one-to-one) with respect to $\mathbf{x}_0 \in \mathcal{X}_0$. This implies that the Jacobian of $\xi(\mathbf{x}_0)$ is full rank, i.e., $\text{rank}\left(\frac{\partial \xi(\mathbf{x}_0)}{\partial \mathbf{x}_0}\right) = n_x \forall \mathbf{x}_0 \in \mathcal{X}_0$. This rank condition is a sufficient condition for uniform observability in \mathcal{X}_0 , a consequence of the real Jacobian conjecture [27].

The following theorem shows that distinguishability along with the observability rank condition are equivalent to uniform observability.

Theorem II.1 ([26], Th. 7): Consider a discrete-time system (2) that satisfies Definition II.1. Such a system satisfies Definition II.3 if there $\exists N_x < N$ such that $\text{rank}\left(\left\{\frac{\partial \mathbf{y}_k}{\partial \mathbf{x}_0}\right\}_{k=0}^{N_x}\right) = n_x \forall \mathbf{x}_0 \in \mathcal{X}_0$.

For discrete-time system (2), the discrete-time flow map can be denoted as $\phi_0^k(\mathbf{x}_0) \equiv \phi_0^{kT}(\mathbf{x}_0) = \mathbf{x}_k$. Such that $\frac{\partial \xi(\mathbf{x}_0)}{\partial \mathbf{x}_0} \in \mathbb{R}^{Nn_y \times n_x}$ for observation horizon N can be computed as

$$\frac{\partial \xi(\mathbf{x}_0)}{\partial \mathbf{x}_0} = \left\{ \frac{\partial \mathbf{y}_k}{\partial \mathbf{x}_0} \right\}_{k=0}^{N-1} = \left\{ \frac{\partial \mathbf{h}(\phi_0^k(\mathbf{x}_0))}{\partial \phi_0^k(\mathbf{x}_0)} \frac{\partial \phi_0^k(\mathbf{x}_0)}{\partial \mathbf{x}_0} \right\}_{k=0}^{N-1}, \quad (5)$$

where $\frac{\partial \phi_0^k(\mathbf{x}_0)}{\partial \mathbf{x}_0} \in \mathbb{R}^{n_x \times n_x}$ is the Jacobian of the flow map (3) with respect to the initial states. We note that Definition II.3 and Theorem II.1 imply that a unique solution exists around \mathbf{x}_0 and therefore imply local observability [10], [26].

B. Empirical Observability Gramian

Considering nonlinear systems, the Empr-Gram is one approach that can be utilized to quantify observability. Within the scope of this note, we focus on the Empr-Gram; definitions and relations to other observability formulations, such as Lie derivatives, are outside the scope of this paper. The discrete-time Empr-Gram $\mathbf{W}_o^\varepsilon(\mathbf{x}_0) \in \mathbb{R}^{n_x \times n_x}$ [5], [8], [9], [28] can be written as

$$\text{Empr-Gram: } \mathbf{W}_o^\varepsilon(\mathbf{x}_0) := \frac{1}{4\varepsilon^2} \sum_{k=0}^{N-1} (\Delta \mathbf{Y}_k^\varepsilon)^\top \Delta \mathbf{Y}_k^\varepsilon, \quad (6)$$

where the impulse response measurement vector $\Delta \mathbf{Y}_k^\varepsilon := \Delta \mathbf{Y}_k^\varepsilon(\mathbf{x}_0) = [\mathbf{y}_k^{+1} - \mathbf{y}_k^{-1}, \dots, \mathbf{y}_k^{+n_x} - \mathbf{y}_k^{-n_x}]^\top \in \mathbb{R}^{n_y \times n_x}$ and $\mathbf{y}_k^{\pm i} = \mathbf{y}_k(\mathbf{x}_0 \pm \varepsilon \mathbf{e}_i, i) \in \mathbb{R}^{1 \times n_y}$. The Gramian (6) is based on initial state impulse response, where $\mathbf{e}_i \in \mathbb{R}^{n_x}$ for $i \in \{1, 2, \dots, n_x\}$ denotes the standard basis vector and $\varepsilon > 0$ is a constant positive infinitesimal parameter. We note here that the horizon for which the Empr-Gram (6) is computed is chosen as N . This choice is based on Definition II.3 of uniform observability and Theorem II.1. It is well-established that the system (2) is locally weakly observable at an initial vector $\mathbf{x}_0 \in \mathcal{X}_0$ if $\lim_{\varepsilon \rightarrow 0} \text{rank}(\mathbf{W}_o^\varepsilon(\mathbf{x}_0)) = n_x$ [28]. Note that the Empr-Gram is considered computationally expensive [10]; it requires simulating the dynamical system (2) from $2n_x$ perturbed initial conditions over the measurement window [18], [29]. The following lemma states that the Empr-Gram is equivalent to the observability rank condition [2] for a LTI system.

Lemma II.1: For any time-invariant linear system (\mathbf{A}, \mathbf{C})

$$\mathbf{x}_{k+1} = \mathbf{A}\mathbf{x}_k, \quad \mathbf{y}_k = \mathbf{C}\mathbf{x}_k, \quad (7)$$

the Empr-Gram reduces to the linear observability Gramian $\mathbf{W}_o^l(\mathbf{x}_0) := \langle \mathbf{O}_l, \mathbf{O}_l \rangle \in \mathbb{R}^{n_x \times n_x}$, where the observability matrix is defined as $\mathbf{O}_l := [\mathbf{C}, \mathbf{C}\mathbf{A}, \dots, \mathbf{C}\mathbf{A}^{N-1}]^\top \in \mathbb{R}^{Nn_y \times n_x}$ for any $\mathbf{x}_0 \in \mathcal{X}_0$ and any infinitesimal $\varepsilon > 0$.

Proof. The proof is analogous to the proofs in [7, Lemma 7] and [8, Lemma 5]. ■

Lemma II.1 indicates that the Empr-Gram is a generalization of the linear Gramian for nonlinear systems. Readers can refer to [2], [12] for additional information on linear observability.

Having briefly introduced the observability notions for nonlinear systems, in the next section we introduce the proposed variational observability Gramian.

III. A VARIATIONAL APPROACH FOR QUANTIFYING NONLINEAR OBSERVABILITY

In this note, we consider the variational system, termed prolonged system in [17], which consists of the variational system along the flow map $\phi_{t_0}^t$. The variational system is written in the following form

$$\delta \dot{\mathbf{x}}(t) = \frac{\partial \mathbf{f}(\phi_{t_0}^t)}{\partial \phi_{t_0}^t} \delta \mathbf{x}(t), \quad \delta \dot{\mathbf{y}}(t) = \frac{\partial \mathbf{h}(\phi_{t_0}^t)}{\partial \phi_{t_0}^t} \delta \mathbf{x}(t), \quad (8)$$

where $\delta \mathbf{x}(t) \in \mathbb{R}^{n_x}$ is the asymptotic time evolution of the states at time t along the system trajectory and $\delta \mathbf{y}(t) \in \mathbb{R}^{n_y}$ is the variational measurement along the system trajectory.

The prolonged system (8) of the original continuous-time nonlinear dynamics (1) can be extended and written as an infinitesimal variational system as presented in [18], [30]. The infinitesimal variational system can be written as

$$\delta \mathbf{x}(t) = \phi_{t_0}^t(\mathbf{x}_0 + \delta \mathbf{x}_0) - \phi_{t_0}^t(\mathbf{x}_0) = \frac{\partial \phi_{t_0}^t(\mathbf{x}_0)}{\partial \mathbf{x}_0} \delta \mathbf{x}_0, \quad (9a)$$

$$\delta \mathbf{y}(t) = \frac{\partial \mathbf{h}(\phi_{t_0}^t(\mathbf{x}_0))}{\partial \phi_{t_0}^t(\mathbf{x}_0)} \frac{\partial \phi_{t_0}^t(\mathbf{x}_0)}{\partial \mathbf{x}_0} \delta \mathbf{x}_0, \quad (9b)$$

where $\delta \mathbf{x}_0 \in \mathbb{R}^{n_x}$ is the infinitesimal perturbation to the initial conditions \mathbf{x}_0 . The variational system (9) is developed by applying the chain rule; readers are referred to [18] for the complete derivation of variational system (9). The following proposition extends the continuous-time variational dynamics (9) into discrete-time variational system representation.

Proposition III.1: The infinitesimal discrete-time variational system representation of the continuous-time variational equations (9) can be written as

$$\delta \mathbf{x}_{k+1} = \Phi_0^k(\mathbf{x}_0) \delta \mathbf{x}_0 = \left(\mathbf{I}_{n_x} + \frac{\partial \tilde{\mathbf{f}}(\mathbf{x}_k)}{\partial \mathbf{x}_k} \right) \frac{\partial \mathbf{x}_k}{\partial \mathbf{x}_0} \delta \mathbf{x}_0, \quad (10a)$$

$$\delta \mathbf{y}_k = \Psi_0^k(\mathbf{x}_0) \delta \mathbf{x}_0 = \frac{\partial \mathbf{h}(\mathbf{x}_k)}{\partial \mathbf{x}_k} \Phi_0^k(\mathbf{x}_0) \delta \mathbf{x}_0, \quad (10b)$$

where $\delta \mathbf{x}_{k+1} \in \mathbb{R}^{n_x}$ is the infinitesimal perturbation at time-index $k+1$ and $\delta \mathbf{y}_k \in \mathbb{R}^{n_y}$ is the variational measurement at time-index k . The discrete-time variational mapping function is defined as $\Phi_0^k(\mathbf{x}_0) := \left(\mathbf{I}_{n_x} + \frac{\partial \tilde{\mathbf{f}}(\mathbf{x}_k)}{\partial \mathbf{x}_k} \right) \frac{\partial \mathbf{x}_k}{\partial \mathbf{x}_0} \in \mathbb{R}^{n_x \times n_x}$ and matrix $\mathbf{I}_{n_x} \in \mathbb{R}^{n_x \times n_x}$ is the identity matrix of size n_x . The variational measurement mapping function is denoted as $\Psi_0^k(\mathbf{x}_0) := \frac{\partial \mathbf{h}(\mathbf{x}_k)}{\partial \mathbf{x}_k} \Phi_0^k(\mathbf{x}_0) \in \mathbb{R}^{n_y \times n_x}$.

Proof. Let $\hat{\mathbf{x}}_0 = \mathbf{x}_0 + \delta \mathbf{x}_0 \in \mathcal{X}_0$, then for any discrete-time index $k > 0$, the state-space equation (2a) can be written as $\hat{\mathbf{x}}_{k+1} = \hat{\mathbf{x}}_k + \tilde{\mathbf{f}}(\hat{\mathbf{x}}_k)$. Analogous to (9), the infinitesimal variational vector for index $k+1$ is rewritten as $\delta \mathbf{x}_{k+1} = \phi_0^{k+1}(\hat{\mathbf{x}}_0) - \phi_0^{k+1}(\mathbf{x}_0) = \hat{\mathbf{x}}_{k+1} - \mathbf{x}_{k+1}$. Applying the definition of Fréchet derivative [31, Definition 3.4.8], i.e., directional derivative, and noting that $\tilde{\mathbf{f}}(\cdot)$ is at least twice differentiable, the following holds true: $\lim_{\delta \mathbf{x}_0 \rightarrow 0} \frac{\hat{\mathbf{x}}_{k+1} - \mathbf{x}_{k+1}}{\hat{\mathbf{x}}_0 - \mathbf{x}_0} = \frac{\hat{\mathbf{x}}_{k+1} - \mathbf{x}_{k+1}}{\mathbf{x}_0 + \delta \mathbf{x}_0 - \mathbf{x}_0} = \frac{\hat{\mathbf{x}}_{k+1} - \mathbf{x}_{k+1}}{\delta \mathbf{x}_0} = \frac{\partial \mathbf{x}_{k+1}}{\partial \mathbf{x}_0}$. Similarly applying the Fréchet derivative to the nonlinear mapping function, we obtain: $\lim_{\delta \mathbf{x}_0 \rightarrow 0} \frac{\tilde{\mathbf{f}}(\hat{\mathbf{x}}_k) - \tilde{\mathbf{f}}(\mathbf{x}_k)}{\hat{\mathbf{x}}_0 - \mathbf{x}_0} = \frac{\partial \tilde{\mathbf{f}}(\mathbf{x}_k)}{\partial \mathbf{x}_0}$; see Appendix A for derivation of $\frac{\partial \tilde{\mathbf{f}}(\mathbf{x}_k)}{\partial \mathbf{x}_0}$. It follows that

$$\delta \mathbf{x}_{k+1} = \underbrace{\hat{\mathbf{x}}_k - \mathbf{x}_k}_{\frac{\partial \mathbf{x}_k}{\partial \mathbf{x}_0} \delta \mathbf{x}_0} + \underbrace{\tilde{\mathbf{f}}(\hat{\mathbf{x}}_k) - \tilde{\mathbf{f}}(\mathbf{x}_k)}_{\frac{\partial \tilde{\mathbf{f}}(\mathbf{x}_k)}{\partial \mathbf{x}_0} \delta \mathbf{x}_0}, \quad (11)$$

then by applying the chain rule, we can write $\frac{\partial \tilde{\mathbf{f}}(\mathbf{x}_k)}{\partial \mathbf{x}_0} = \frac{\partial \tilde{\mathbf{f}}(\mathbf{x}_k)}{\partial \mathbf{x}_k} \frac{\partial \mathbf{x}_k}{\partial \mathbf{x}_0}$, the rest requires factoring out $\frac{\partial \mathbf{x}_k}{\partial \mathbf{x}_0}$. Using an analogous approach, the variational measurement vector $\delta \mathbf{y}_k$ for any $k > 0$ can be written as

$$\delta \mathbf{y}_k = \hat{\mathbf{y}}_k - \mathbf{y}_k = \frac{\partial \mathbf{y}_k}{\partial \mathbf{x}_0} \delta \mathbf{x}_k = \frac{\partial \mathbf{h}(\mathbf{x}_k)}{\partial \mathbf{x}_k} \frac{\partial \mathbf{x}_k}{\partial \mathbf{x}_0} \delta \mathbf{x}_0, \quad (12)$$

then, substituting the above with the variational state vector $\delta \mathbf{x}_k$ we obtain (10). This completes the proof. ■

For ease of notation, we refer to $\mathbf{x}_k \equiv \phi_0^k$ and remove the dependency of $\Phi_0^k(\mathbf{x}_0) = \Phi_0^k$ and $\Psi_0^k(\mathbf{x}_0) = \Psi_0^k$ on \mathbf{x}_0 .

Remark III.1: The variational mapping function Φ_0^k requires the knowledge of states \mathbf{x}_i for $i \in \{0, 1, \dots, k\}$. Notice that this function can be written as $\Phi_0^k = \frac{\partial \phi_0^k}{\partial \phi_0^{k-1}} \frac{\partial \phi_0^{k-1}}{\partial \mathbf{x}_0}$. Now, computing Φ_0^k requires evaluation under the chain rule and thus can be written for any discrete-time index k as

$$\Phi_0^k = \Phi_{k-1}^k \Phi_{k-2}^{k-1} \cdots \Phi_0^1 \Phi_0^0 = \prod_1^{i=k} \Phi_{i-1}^i, \quad (13)$$

where matrix $\Phi_{i-1}^i = \frac{\partial \phi_0^i}{\partial \phi_0^{i-1}} \frac{\partial \phi_0^{i-1}}{\partial \phi_0^{i-1}}$ represents the partial derivatives with respect to ϕ_0^{i-1} . Given that $\Phi_0^0 = \frac{\partial \mathbf{x}_0}{\partial \mathbf{x}_0}$ is equal to an identity matrix \mathbf{I}_{n_x} ; it is removed for simplicity of notation.

Having formulated the discrete-time variational system, we now introduce the proposed observability Gramian according to the following proposition.

Proposition III.2: Consider a variational discrete-time system (10) with measurement model. Following the results of Theorem II.1, there exists a finite-time measurement horizon $N \in \mathbb{N}$, such that the variational observability Gramian evaluated around initial state $\mathbf{x}_0 \in \mathcal{X}_0$ can be expressed as

$$\text{Var-Gram: } \mathbf{V}_o(\mathbf{x}_0) := \Psi(\mathbf{x}_0)^\top \Psi(\mathbf{x}_0) \in \mathbb{R}^{n_x \times n_x}, \quad (14)$$

where observability matrix $\Psi(\mathbf{x}_0) := \Psi \in \mathbb{R}^{N n_y \times n_x}$ concatenates the variational observations $\delta \mathbf{y}_k$ over measurement horizon N for $k \in \{0, 1, \dots, N-1\}$ and can be written as

$$\Psi := [\Psi_0^0, \Psi_0^1, \Psi_0^2, \dots, \Psi_0^{N-1}]^\top. \quad (15)$$

Note that Ψ_0^k is the variational measurement mapping function defined in (10b). For $k=0$, we have $\Psi_0^0 = \frac{\partial \mathbf{h}(\mathbf{x}_0)}{\partial \mathbf{x}_0} \Phi_0^0$, such that Φ_0^0 is equal \mathbf{I}_{n_x} .

Proof. Theorem II.1 implies the existence of an output sequence over a finite-time horizon, such that a unique solution around $\mathbf{x}_0 \in \mathcal{X}_0$ exists. With that in mind, we show that measurement vector (15) is equivalent to the Jacobian of the sequence $\xi(\mathbf{x}_0)$. This equivalence shows that Var-Gram (14) represents the observability Gramian of the variational system. It follows from (10), by applying the chain rule as discussed in Remark III.1, that (15) can be rewritten as

$$\Psi = \left\{ \frac{\partial \mathbf{h}(\mathbf{x}_k)}{\partial \mathbf{x}_k} \Phi_0^k \right\}_{k=0}^{N-1} = \left\{ \frac{\partial \mathbf{h}(\mathbf{x}_k)}{\partial \mathbf{x}_k} \prod_1^{i=k} \Phi_{i-1}^i \right\}_{k=0}^{N-1}, \quad (16)$$

we use column notation to express a matrix concatenated from iterated matrix entries for $k \in \{0, 1, \dots, N-1\}$. Referring to Definition II.3, $\frac{\partial \xi(\mathbf{x}_0)}{\partial \mathbf{x}_0} = \left\{ \frac{\partial \mathbf{h}(\phi_0^k(\mathbf{x}_0))}{\partial \phi_0^k(\mathbf{x}_0)} \frac{\partial \phi_0^k(\mathbf{x}_0)}{\partial \mathbf{x}_0} \right\}_{k=0}^{N-1}$; see (5). The partial derivative $\frac{\partial \phi_0^k(\mathbf{x}_0)}{\partial \mathbf{x}_0}$ reduces to the Jacobian of the discrete-time state-equation (2a). Under the action of the chain rule it can be expressed as $\left(\mathbf{I}_{n_x} + \frac{\partial \tilde{\mathbf{f}}(\mathbf{x}_k)}{\partial \mathbf{x}_k} \right) \frac{\partial \phi_0^k(\mathbf{x}_0)}{\partial \mathbf{x}_0}$. It is now clear that (15) and (4) are equivalent. As such, the proof is complete. ■

Based on Proposition III.2, we now show that the proposed Var-Gram (14) for nonlinear systems reduces to the linear observability Gramian.

Corollary III.1: For any LTI system satisfying Assumption II.1, the observability Gramian in (14) reduces to the linear observability Gramian $W_o^l(x_0)$.

Proof. For a LTI system with linear measurement mapping $\frac{\partial h(x_k)}{\partial x_k} = C \forall k \in \{0, 1, \dots, N-1\}$ and under the action of the chain rule as discussed in Remark III.1, the variational measurement equation (10b) reduces to the following

$$\Psi_0^k = \frac{\partial h(x_k)}{\partial x_k} \Phi_0^k = C \prod_{i=k}^1 \Phi_{i-1}^i, \quad (17)$$

where Φ_0^k is equivalent to A^k for any $k \in \{0, 1, \dots, N-1\}$. Given that A^k is invariant along the system trajectory. It follows that for a LTI system, the variational observability matrix reduces to the linear observability matrix as follows

$$\Psi = O_l = [C, CA, \dots, CA^{N-1}]^\top; \text{ refer to (15).}$$

As such, while noting that the multiplication of any matrix-valued vector with its transpose is equivalent to its matrix dot-product, the following holds true

$$V_o(x_0) = \Psi^\top \Psi = \langle \Psi, \Psi \rangle \equiv \langle O_l, O_l \rangle = W_o^l(x_0). \quad (18)$$

The proof is therefore complete. ■

Having established the above relation to the linear observability Gramian, we now relate the introduced Var-Gram (14) to the Empr-Gram (6) for nonlinear dynamical systems.

Theorem III.1: Consider the discrete-time nonlinear mapping functions $\tilde{f}(\cdot)$ and $h(\cdot)$ under the condition of differentiability. The Empr-Gram (6), for any sufficiently small $\epsilon > 0$, is equivalent to the proposed Var-Gram (14) for any initial conditions satisfying Assumption II.1.

Proof. For proof of Theorem III.1, see Appendix B. ■

Theorem III.1 demonstrates that the Var-Gram, based on the infinitesimal variational system (10), is a model-based equivalent formulation of the impulse response Empr-Gram. It is worthwhile to note that the Empr-Gram, although computed from simple algebraic operations, requires $2n_x$ impulse response simulations to construct. Alternatively, the Var-Gram, which relies on variational dynamics, is computed along one local trajectory for any $x_0 \in \mathcal{X}_0$. A comparison of computational effort is illustrated in Section VI. It is also important to note that the Var-Gram, directly computed from the variational dynamics, which depicts local variations along the system trajectory, is dynamical scaled to account for such variations. Nevertheless, this is not true for the Empr-Gram which requires studying the states and output measurements to properly scale internal states relative to size of eigenvalues of the Empr-Gram [5]. We note here that the Var-Gram requires that the nonlinear mapping functions $\tilde{f}(\cdot)$ and $h(\cdot)$ to be smooth and at least twice differentiable, while the Empr-Gram requires the system to be only numerically integrable.

IV. OBSERVABILITY CONDITIONS & LYAPUNOV EXPONENTS

There exist several observability measures and metrics that can be defined based on the rank, smallest eigenvalue, condition number, trace, and determinant of an observability

Gramian—see [32], [33] and references therein. In this section, we show evidence of connections between observability measures related to the proposed observability Gramian and Lyapunov exponents.

Lyapunov exponents measure the exponential rate of convergence and divergence of nearby orbits of an attractor in the state-space [34]. The exponents provide a characteristic spectrum that offers a basis for stability notions introduced in Lyapunov's work on the problem of stability of motions [13]. In such context, δx_0 is considered an infinitesimal perturbation $\epsilon > 0$ to initial conditions x_0 and its exponential decay or growth is denoted as δx_k .

Calculating Lyapunov exponents is well-established within the literature [16], [34]. For nonlinear Lyapunov exponents calculation, we consider the infinitesimal discrete-time variational representation (10) of the nonlinear dynamics in (3); see [23] for complete derivation of such representation within the field of chaos and ergodicity.

Given a discrete-time flow map for a given trajectory $\phi_0^k \in \mathcal{X}$ starting from initial point $x_0 \in \mathcal{X}_0$, the finite-time Lyapunov exponents are defined as

$$\lambda_L(x_0) := \lim_{k \rightarrow N} \frac{1}{k} \log \left(\frac{\|\delta x_k\|}{\|\delta x_0\|} \right) = \lim_{k \rightarrow N} \frac{1}{k} \log (\|\Phi_0^k\|), \quad (19)$$

where $\lambda_L(x_0) := \lambda_L \in \mathbb{R}^{n_x \times n_x}$ is a matrix having the Lyapunov exponents on the diagonal. The norms $\|\delta x_k\|$ and $\|\delta x_0\|$ represent the average magnitude of the perturbation on x_k and x_0 . The induced norm $\|\Phi_0^k\| \in \mathbb{R}^{n_x \times n_x}$ represents the deformation of an infinitesimal volume; its square is termed the Cauchy-Green deformation matrix—see [15], [35].

For continuous-time systems it is typical to assume the assumption of regularity; see [16], [36]. This is essential for the existence and stability of the Lyapunov spectrum of exponents under small perturbation. However, for the case of discrete-time systems, such regularity is implied from *Oseledec's ergodicity theorem* that was proven in the late 1960s [16].

Remark IV.1: The regularity of the dynamical system (2) is a mild condition. The existence of the full spectrum of LEs is well-established as a result of the multiplicative ergodic theorem (Oseledec's Theorem); see [16, Section 10.1].

It follows that for systems in discrete-time, Oseledec's splitting fully decomposes Lyapunov vectors and therefore guarantees the existence of a full Lyapunov spectrum of Exponents [16], [30], [36]–[38]. This result eliminates the technical challenges of computing the LEs while requiring the verification of system regularity, defined by the existence and smoothness of variational mapping functions Φ_0^k .

The following lemma is essential for establishing connections between Lyapunov exponents and observability measures that are based on the proposed Var-Gram.

Lemma IV.1 ([16]): The following properties hold true for Lyapunov exponents λ_L [16, Theorem 2.1.2]:

$$(L2.1) \quad \lambda_L(\beta A) = \lambda_L(A) \forall \beta \in \mathbb{R} \setminus \{0\},$$

$$(L2.2) \quad \lambda_L(A_1 + A_2) \leq \max\{\lambda_L(A_1), \lambda_L(A_2)\}.$$

The matrix A represents the system's deformation matrix along a trajectory. Based on Lemma IV.1, in the following,

we illustrate that the log-det of the proposed Var-Gram (14) is related to the system's Lyapunov exponents (19).

Theorem IV.1: Let the Var-Gram be defined as (14) and the Lyapunov spectrum of exponents as (19). The log-det of the Var-Gram has an underlying connection to the Lyapunov spectrum of exponents according to the following

$$\log\text{-det}(\mathbf{V}_o(\mathbf{x}_0)) \equiv \alpha \sum_{i=1}^{n_x} \lambda_{L,i}, \quad (20)$$

where $\lambda_{L,i}$ are the Lyapunov exponents, i.e., the eigenvalues of diagonal matrix λ_L , and the constant $\alpha = 2N$.

Proof. The proof of Theorem IV.1 for a linear measurement model is available in Appendix B. ■

Theorem V.1 provides evidence that the Var-Gram is modular, which in turn implies the submodularity of the log-det observability measure; see Corollary V.1. This submodularity is a direct consequence of the modularity of the proposed Gramian. Having provided the above relation between the proposed Var-Gram measure and Lyapunov exponents, the following theorem illustrates a local observability condition for discrete-time nonlinear systems without inputs.

Theorem IV.2: For any discrete-time nonlinear system (2) satisfying Assumption II.1 and regularity, the system is said to be uniformly observable around $\mathbf{x}_0 \in \mathcal{X}_0$ if for a finite-time horizon $N \in \mathbb{N}$ and for $\mathbf{V}_o(\cdot) \succeq 0$ it holds true that

$$\rho(\mathbf{V}_o) = \sup \lim_{k \rightarrow N} \frac{1}{2^k} \mathbf{V}_o(\mathbf{x}_0) < 1, \quad (21)$$

where $\rho(\mathbf{V}_o)$ is the spectral radius of the proposed Gramian.

Proof. The proof follows from Theorem IV.1, where the Gramian (14) is shown to be equivalent to the Lyapunov exponents according to (20). The exponents denote the exponential asymptotic stability around an ellipsoid $\delta\mathbf{x}_0$ along the trajectory \mathbf{x}_k . This translates into having the spectral radius of the Lyapunov exponents $\rho(\lambda_L) < 0$. Now, noting that if the Lyapunov exponents are positive $\lambda_{L,i} > 0$, the vectors formed from the intersection of $\Phi_0^k \cap \Phi_0^1 = 0$; refer to [39, Th.2.4]. This indicates that there is a loss of information along the trajectory from time index 0 to k .

Note that Φ_0^k is iteratively calculated based on Φ_0^1 (Remark III.1), it follows that the Var-Gram cannot be computed for the aforementioned condition [39, Th.2.4]. Based on the equivalence relation provided in theorem IV.1, the Lyapunov exponents are to be strictly negative. Now given that $\lambda_L \equiv \frac{1}{2^k} \log(\mathbf{V}_o)$, it implies that the maximal eigenvalue of the Var-Gram is to be strictly $\mathbf{V}_o < 1$. This corresponds to the spectral radius being strictly less than 1. ■

The following corollary provides necessary and sufficient conditions for the local observability of nonlinear system (2) represented in discrete-time variational form (10).

Corollary IV.1: Let $\mathbf{V}_o(\cdot) = \Psi(\mathbf{x}_0)^\top \Psi(\mathbf{x}_0)$ denote the Var-Gram computed for the variational system (10). The spectral radius $\lim_{k \rightarrow \infty} \sup \|\Psi_0^k\|^{\frac{1}{k}} \leq 1$ if and only if there exists a constant K such that $\|\Psi_{k-1}^k \Psi_{k-2}^{k-1} \cdots \Psi_0^1\| \leq K$ for all $k \in \{0, 1, \dots, N-1\}$.

Proof. The equivalence between the boundedness of a matrix product norm and the spectral radius condition is

established in [40]. The proof follows from the subadditivity property and the equivalence of norms [40, Lemma 1]. ■

Theorem IV.1 shows that the log-det of the var-Gram is equivalent to computing the Lyapunov exponents of a system. The latter being a computationally tractable given the fact that it can be computed through data-driven approaches [34]. As such, this equivalence provides data-driven prospects for observability quantification. Theorem IV.2 provides a uniform observability condition around \mathbf{x}_0 for assessing the observability of discrete-time nonlinear systems. Such observability condition can be used in the context of sensor selection and state-estimation.

The condition presented in Corollary IV.1 holds true for discrete nonlinear systems under Assumption II.1 and with the regularity of the system (10); see Remark IV.1. The condition of regularity established by the multiplicative ergodic theorem ensures the boundedness of Φ_0^k and $\Psi_0^k \forall k \in \{0, 1, \dots, N-1\}$ and thus the existence of a finite joint spectral radius (Corollary IV.1). The spectral radius limit in turn presents necessary conditions for local uniform observability (Definition II.3).

In the subsequent section, we introduce the observability-based SNS framework that relies on submodular measures pertaining to the proposed variational Gramian.

V. APPLICATION OF OBSERVABILITY-BASED SNS IN NONLINEAR NETWORKS

The interdependence between internal states allows for the reconstruction of system states by measuring a subset of the total states. This formulates the basis of observability-based SNS for dynamical systems. While myriad methods exist for addressing the SNS problem in linear systems, approaches for nonlinear systems are less developed. One approach for posing the observability-based SNS problem in nonlinear networks involves formulating it as a constraint set maximization problem; refer to [33]—see [41], [42] and references therein for other approaches.

To that end, we define the *set function* $\mathcal{O}(\mathcal{S}) : 2^{\mathcal{V}} \rightarrow \mathbb{R}$ with $\mathcal{V} := \{i \in \mathbb{N} \mid 0 < i \leq n_y\}$. The set \mathcal{V} denotes all the possible sets of sensor locations combinations and set \mathcal{S} represents a set of sensor combinations such that $\mathcal{S} \subseteq \mathcal{V}$. As such, the SNS set optimization problem can be written as

$$(\mathbf{P1}) \quad \mathcal{O}^*(\mathcal{S}) := \underset{\mathcal{S} \subseteq \mathcal{V}}{\text{maximize}} \quad \mathcal{O}(\mathcal{S}), \quad \text{subject to} \quad |\mathcal{S}| = r. \quad (22)$$

In the context of applications to optimal SNS, solving **P1** refers to finding the best sensor configuration \mathcal{S} containing r number of sensors whereby an observability-based metric $\mathcal{O}(\mathcal{S})$ is maximized. The rationale for posing the SNS problem as a set optimization problem is based on the properties of the observability set function. Such that the underlying set function properties (modularity and submodularity) allow for a scalable solution to the SNS problem. The following are definitions of modular and submodular set functions.

Definition V.1 (modularity [43]): A set function $\mathcal{O} : 2^{\mathcal{V}} \rightarrow \mathbb{R}$ is said to be modular if and only if for any $\mathcal{S} \subseteq \mathcal{V}$ and weight function $w : \mathcal{V} \rightarrow \mathbb{R}$, it holds that $\mathcal{O}(\mathcal{S}) = w(\emptyset) + \sum_{s \in \mathcal{S}} w(s)$.

Definition V.2 (submodularity [43]): A set function $\mathcal{O} : 2^{\mathcal{V}} \rightarrow \mathbb{R}$ is said to be submodular if and only if for any

$\mathcal{A}, \mathcal{B} \subseteq \mathcal{V}$ given that $\mathcal{A} \subseteq \mathcal{B}$, it holds that for all $s \notin \mathcal{B}$

$$\mathcal{O}(\mathcal{A} \cup \{s\}) - \mathcal{O}(\mathcal{A}) \geq \mathcal{O}(\mathcal{B} \cup \{s\}) - \mathcal{O}(\mathcal{B}). \quad (23)$$

There are several observability measures that enable the quantification of a dynamical system's observability. These measures are typically based on the rank, smallest eigenvalue, trace, and determinant of an observability matrix—see [32], [33] and references therein. We note that for the chosen observability measure function, that is log-det, the SNS problem **P1** which is based on the proposed Var-Gram is rendered submodular and monotone increasing*. This is analogous to the case for a linear Gramians, as shown in [33]. Recall that the variational form (10) of a discrete-time system represents the system flow along the tangent space which is a linear space. Furthermore, the choice of network-based observability measure, log-det is due to its underlying connection to Lyapunov exponents; see Theorem IV.1.

Before introducing Theorem V.1 and its Corollary V.1, which demonstrate the modularity of the Var-Gram and the submodularity of the log-det observability measure, we define parameterization matrix $\mathbf{\Gamma} := \text{diag}\{\gamma_j\}_{j=1}^{n_y} \in \mathbb{R}^{n_y \times n_y}$ as the matrix that determines the allocation of the sensors. Such that, a node j is equipped with a sensor if $\gamma_j = 1$. Otherwise, γ_j is set to 0. We also define the parameterized vector γ that represents the sensor selection, i.e., a column vector $\gamma := \{\gamma_j\}_{j=1}^{n_y}$. The measurement mapping function $\mathbf{h}(\mathbf{x}_k)$ can then be defined as $\mathbf{h}(\mathbf{x}_k) := \mathbf{\Gamma} \mathbf{C} \mathbf{x}_k$. Note that for **P1**, the variable $\mathbf{\Gamma}$ is encoded in the set \mathcal{S} , such that for each sensor node a value of γ_j is attributed to the set \mathcal{S} at location j . The following proposition demonstrates that the proposed Var-Gram under the context of SNS is a modular set function.

Theorem V.1: The Var-Gram $\mathbf{V}_o(\mathcal{S}, \mathbf{x}_0) := \mathbf{V}_o(\mathcal{S}) \in \mathbb{R}^{n_x \times n_x}$ defined by

$$\mathbf{V}_o(\mathcal{S}) = \mathbf{\Psi}(\mathcal{S})^\top \mathbf{\Psi}(\mathcal{S}), \quad (24)$$

for $\mathcal{S} \subseteq \mathcal{V}$ is a modular set function under parameterization γ .

Proof. For the proof of Theorem V.1, see Appendix B. ■

Notice that from Definition V.1, the Var-Gram is considered a linear mapping function with respect to the sensor selection parameterization vector γ . To that end, in the following proposition, we establish the submodularity of the Var-Gram observability-based measure $\mathcal{O}(\mathcal{S})$.

Corollary V.1: Let $\mathcal{O}(\mathcal{S}) : 2^{\mathcal{V}} \rightarrow \mathbb{R}$ be a set function defined as

$$\mathcal{O}(\mathcal{S}) := \log\text{-det}(\mathbf{V}(\mathcal{S})), \quad (25)$$

for $\mathcal{S} \subseteq \mathcal{V}$. Then $\mathcal{O}(\mathcal{S})$ is a submodular monotone increasing set function.

Proof. Let $\mathcal{O}_s : 2^{V-\{s\}} \rightarrow \mathbb{R}$ denote a derived set function defined as

$$\begin{aligned} \mathcal{O}_s(\mathcal{S}) &= \log\text{-det} \mathbf{V}_o(\mathcal{S} \cup \{s\}) - \log\text{-det} \mathbf{V}_o(\mathcal{S}), \\ &= \log\text{-det}(\mathbf{V}_o(\mathcal{S}) + \mathbf{V}_o(\{s\})) - \log\text{-det} \mathbf{V}_o(\mathcal{S}). \end{aligned}$$

We first show $\mathcal{O}_s(\mathcal{S})$ is monotone decreasing for any $s \in V$. That being said, let $\mathcal{A} \subseteq \mathcal{B} \subseteq \mathcal{V} - \{s\}$, and let $\mathbf{V}_o(\tilde{\mathbf{c}}) = \mathbf{V}_o(\mathcal{A}) + \tilde{\mathbf{c}}(\mathbf{V}_o(\mathcal{B}) - \mathbf{V}_o(\mathcal{A}))$ for $\tilde{\mathbf{c}} \in [0, 1]$. Then for

*Let $\mathcal{O} : 2^{\mathcal{V}} \rightarrow \mathbb{R}$ denote a set function. For any $\mathcal{A}, \mathcal{B} \subseteq \mathcal{V}$, the set function is monotone increasing if, for $\mathcal{A} \subseteq \mathcal{B}$ the following is true, $f(\mathcal{B}) \geq f(\mathcal{A})$.

$$\tilde{\mathcal{O}}_s(\mathbf{V}_o(\tilde{\mathbf{c}})) = \log\text{-det}(\mathbf{V}_o(\tilde{\mathbf{c}}) + \mathbf{V}_o(\mathcal{S})) - \log\text{-det}(\mathbf{V}_o(\tilde{\mathbf{c}})),$$

we obtain the following

$$\frac{d}{d\tilde{\mathbf{c}}} \tilde{\mathcal{O}}_s(\mathbf{V}_o(\tilde{\mathbf{c}})) = \text{trace} \left[\left((\mathbf{V}_o(\tilde{\mathbf{c}}) + \mathbf{V}_o(\mathcal{S}))^{-1} - \mathbf{V}_o(\tilde{\mathbf{c}})^{-1} \right) (\mathbf{V}_o(\mathcal{B}) - \mathbf{V}_o(\mathcal{A})) \right] \leq 0.$$

Such that $\left((\mathbf{V}_o(\tilde{\mathbf{c}}) + \mathbf{V}_o(\mathcal{S}))^{-1} - \mathbf{V}_o(\tilde{\mathbf{c}})^{-1} \right)^{-1} \succeq 0$, and $(\mathbf{V}_o(\mathcal{B}) - \mathbf{V}_o(\mathcal{A})) \succeq 0$, then the above inequality holds. We have therefore shown that $\mathcal{O}(\mathcal{S})$ is submodular and \mathcal{O}_s is monotone decreasing. Then, by the additive property of $\mathbf{V}_o(\mathcal{S})$ (see [33]) we have $\mathcal{O}(\mathcal{S})$ being monotone increasing. The proof is analogous and a corollary to the results in [33, Theorem 6] and [44, Lemma 3]. ■

Theorem V.1 provides evidence that the Var-Gram is modular, which in turn implies the submodularity of the log-det observability measure; see Corollary V.1. This submodularity is a direct consequence of the modularity of the proposed Gramian.

Remark V.1: Notice that, for the log-det to be submodular and monotone increasing, the variational observability Gramian can have zero eigenvalues.

In study [44], the considered observability measures are based on the Lie derivative matrix \mathbf{O}_l . That being said, the above submodular properties hold true if and only if \mathbf{O}_l is full rank. In this case when considering the variational Gramian, there is no such restriction. The submodularity of the log det still holds in rank deficient situations. Such situations can arise when not enough sensing nodes are chosen and thereby the system is not yet fully observable.

It is worthwhile to note that the set optimization problem **P1** for a log-det measure results in a submodular set optimization problem. Having a submodular set function allows to exploit computationally tractable algorithms to solve **P1**. Typically, a greedy algorithm, with a running time complexity of $\mathcal{O}(|\mathcal{S}||\mathcal{V}|)$, is employed to solve the submodular problem—see [11, Algorithm 1] for the algorithm. The algorithm has a theoretical performance guarantee, as provided in the following theorem.

Theorem V.2: ([45]) Let $\mathcal{O} : 2^V \rightarrow \mathbb{R}$ be a submodular monotone increasing function, \mathcal{O}^* be the optimal solution of the SNS problem and \mathcal{O}_s^* be the solution obtained from the greedy algorithm. Then, the following performance bound holds true

$$\mathcal{O}_s^* - \mathcal{O}(\emptyset) \geq \left(1 - \frac{1}{e}\right) (\mathcal{O}^* - \mathcal{O}(\emptyset)), \quad \text{with } \mathcal{O}(\emptyset) = 0.$$

This approach achieves a $(1 - 1/e)$ performance guarantee. Given that $(1 - 1/e) \approx 0.63$, \mathcal{O}_s^* is at least 0.63 the optimal value \mathcal{O}^* . Note that for submodular set maximization problems, an accuracy of 99% can be achieved [33]. As mentioned earlier, the proposed observability Gramian, which is based on a variational model that belongs to a linear tangent space, enables the application of algorithms developed for linear Gramians. The evidence of modularity of the Var-Gram (Theorem V.1) provides a rational for submodular set maximization under SNS in nonlinear networks.

TABLE I
COMPUTATIONAL TIME FOR COMPUTING THE OBSERVABILITY GRAMIANS.

Network	Perturbation α_L	Computational Time (s)	
		Var-Gram	Empr-Gram
H ₂ O ₂	20%	0.0043	7.38
	30%	0.0032	8.53
GRI30	20%	0.489	115.05
	30%	0.467	112.06

VI. NUMERICAL CASE STUDIES

In this paper, we introduce a variational Gramian for discrete nonlinear systems of the form (2). To demonstrate the effectiveness of the proposed method, we investigate the following research questions.

- (Q1) Theorem III.1 establishes the equivalence between the Var-Gram and Empr-Gram. Is the equivalence formulated in Theorem III.1 numerically valid? With that in mind, does the Var-Gram dynamically depict the intrinsic relations between the states and is it computationally more tractable than the Empr-Gram?
- (Q2) Does the established observability condition presented in Theorem IV.2 hold true for the system under study?
- (Q3) Having provided evidence regarding the modularity of the Var-Gram, does solving P1 result in optimal sensor node selections? Is the proposed optimal SNS problem scalable for larger nonlinear networks?

We consider a nonlinear combustion reaction network [46] with a state-space formulation of the following form

$$\dot{\mathbf{x}}(t) = \Theta \psi(\mathbf{x}(t)), \quad (26)$$

where $\psi(\mathbf{x}) = [\psi_1(\mathbf{x}), \psi_2(\mathbf{x}), \dots, \psi_{n_r}(\mathbf{x})]^T$, such that ψ_j , $j = \{1, 2, \dots, N_r\}$ are the polynomial functions of concentrations. State vector $\mathbf{x} = [x^1, x^2, \dots, x^{n_x}]$, represents the concentrations of n_x chemical species. The constant matrix $\Theta = [w_{ji} - q_{ji}] \in \mathbb{R}^{n_x \times N_r}$, where q_{ji} and w_{ji} are stoichiometric coefficients. The number of chemical reactions is denoted by N_r and the list of reactions can be written as $\sum_{i=1}^{n_x} q_{ji} \mathcal{R}_i \rightleftharpoons \sum_{i=1}^{n_x} w_{ji} \mathcal{R}_i$, $j \in \{1, 2, \dots, N_r\}$, where \mathcal{R}_i , $i \in \{1, 2, \dots, n_x\}$ are the chemical species.

We study two combustion reaction networks: (N1) an H₂O₂ network that has $N_r = 27$ reactions and $n_x = 9$ chemical species and (N2) a GRI30 network that has $N_r = 325$ reactions and $n_x = 53$ chemical species. For specifics regarding system parameters and definitions, we refer the readers to our previous work [11, Section V]. The discretization constant is $T = 1 \cdot 10^{-12}$ and observation window of $N = 1000$ is chosen. The choice of discretization constant is a result of analyzing the system's initial condition response. For the computation of Empr-Gram, the constant ε is chosen as $\varepsilon = 10^{-4}$.

A. Observability of a Combustion Reaction Network

Given the scope of this work, we examine the proposed Gramian and present a comparison to the Empr-Gram. The comparison between the studied Gramians for H₂O₂ network is depicted in Fig. 1. For brevity, we did not include the observability matrix for GRI30 network. It is clear that the

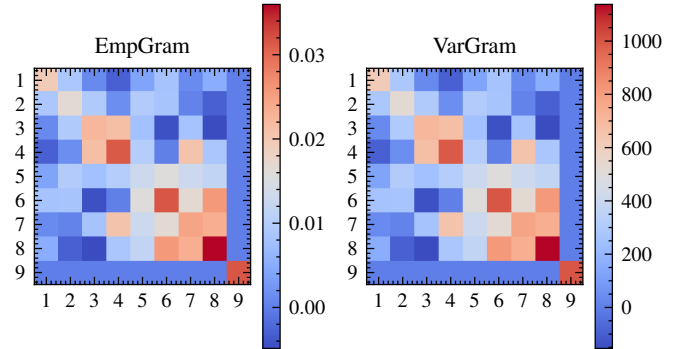


Fig. 1. Mapping of the Empirical (left) and proposed (right) observability Gramians. The square colors indicate the strength and direction of the relations between the variables. Color contrast represents strength while the color itself represents the direction of interrelations.

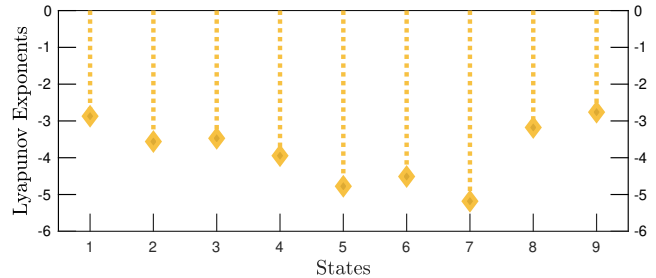


Fig. 2. Lyapunov exponents computed for the H₂O₂ reaction network.

interrelation between the variables is equivalent for the two Gramian formulations. The depicted equivalence is a consequence of Theorem III.1. However, as mentioned earlier [5], the Empr-Gram requires the heuristic scaling of measurement and state variables. This is evident by the strength or amplitude of the state interrelations which is the magnitude of $\{10^{-3}\}$; it is dynamically scaled to a magnitude of $\{10^3\}$ in the Var-Gram. This is important since under a dynamic system response, any small perturbations to initial conditions can appear naturally in the Gramian formulation.

Having numerically validated the equivalence mentioned above, we now present numerical evidence demonstrating the computational efficiency of the proposed method compared to the Empr-Gram. To that end, the computational time required to compute the Var-Gram and the Empr-Gram for both combustion networks N1 and N2 under different perturbations α_L to initial conditions \mathbf{x}_0 is presented in Tab. I. Perturbation term α_L is applied to simulate the system under different transient conditions. It is clear that the Var-Gram is more amenable for scaling for larger nonlinear networks due to its lower computational cost. The reason is that the Var-Gram does not require evaluating the response of the dynamical system (10) from $2n_x$ initial conditions, whereas the Empr-Gram requires a more extensive computational effort by requiring system impulse response evaluation from each of these initial conditions. The aforementioned observations answer the posed questions in Q1.

Fig. 2 depicts the value of the Lyapunov exponents for the H₂O₂ combustion network. The results show, as indicated by the direction of the dotted lines and the location of the diamond markers, that the exponents $\lambda_{L,i} < 0$ are all negative and therefore satisfying the observability condition presented in

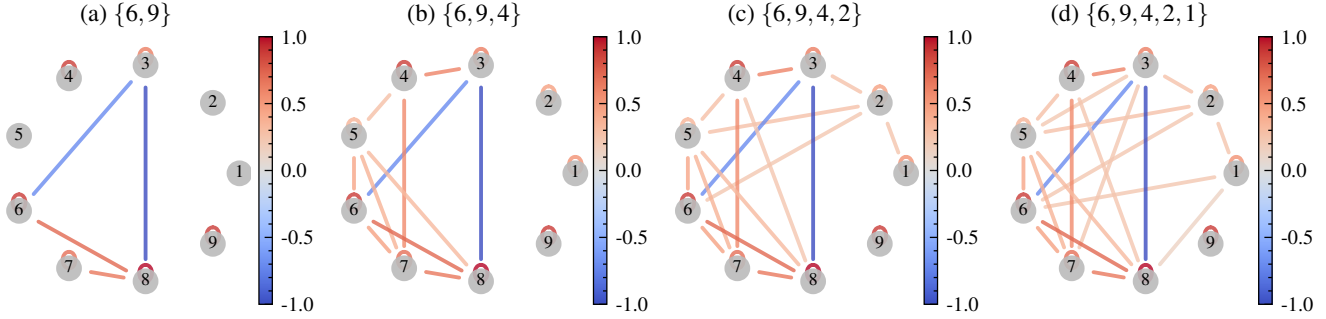


Fig. 3. Optimally selected subset of sensor nodes for the H_2O_2 combustion network under sensor ratios $r = [2, 3, 4, 5]/9$. Sub-figures (a)-(d) depict the sequential order of sensor selections and the corresponding nodes observed. The normalized observability relation between state variables is indicated by the edge color contrast for each sensor ratio. The color intensity represents the strength of observability.

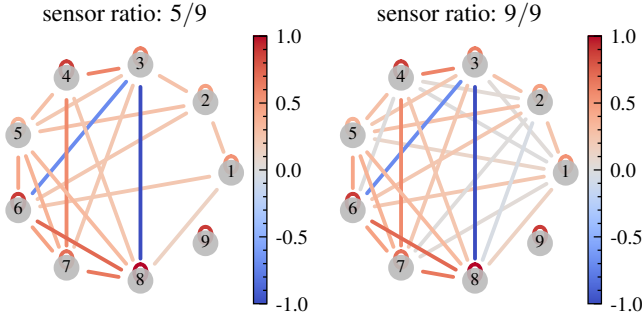


Fig. 4. Normalized observability relation between state variables based on $(5/9 \equiv 0.7)$ sensor node ratio (left) and full node sensor ratio (right) for the sensed nodes within the nonlinear combustion network. For left figure, sensed nodes are optimally chosen as $\{1, 2, 4, 6, 9\}$.

Theorem IV.2. This is true as a consequence of Theorem IV.1, since for any λ_i value less than 1, the Lyapunov exponents $\log \lambda_i = \lambda_{L,i} < 0$, i.e., are strictly negative. This verifies that the system is observable when considering $|\mathcal{S}| = n_x$, i.e., the system has sensors employed on all sensor nodes. As such, the condition posed in research question Q2 holds true for the considered combustion network.

B. Sensor Node Selection in Nonlinear Networks

The greedy algorithm [11, Algorithm 1] is employed to solve the SNS problem **P1** with (25) as the submodular objective function. We solve the optimal SNS problem for combustion networks $N1$ and $N2$ using the log-det measure. The sensor ratios chosen are $[0.4, 0.5, 0.6, 0.7] \times n_x$. For H_2O_2 network this is equivalent to sensors $r = [2, 3, 4, 5]$. The results for SNS on $N1$ for each of the sensor ratios are depicted in Fig. 3. The figure depicts the order of which the sensors are allocated when increasing the sensor ratio and the respective normalized internal state relations between the states. For instance, when observing nodes $\{6, 9\}$, the states $\{3, 7, 8\}$ can be inferred due to the internal state connections with 6. Notice that node 9 has a self-loop thereby indicating that it is a non-interacting chemical species. This means that node 9 is only observable when the same node is selected. The optimally selected subset of the sensor nodes is $\{1, 2, 4, 6, 9\}$ for H_2O_2 network under a sensor number $r = 5$. To validate the optimally selected set refer to Fig. 4 which depicts the normalized internal state relations for sensor ratio 5/9 and that of a full sensor selection ratio. Note that the normalization is based on a min-max normalization process which results in

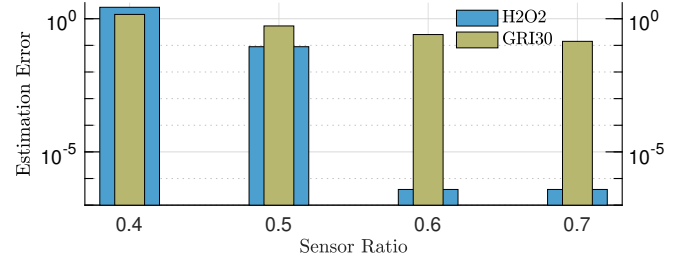


Fig. 5. State estimation error based on the optimal SNS set \mathcal{S}^* . The performance of the state estimation depends on the degree of system observability.

a normalized observability relation ranging between $\{-1, 1\}$. The strength of the state relations and interactions for both sensor fractions allow for internal state connection between all the states thereby indicating the optimality of the chosen sensor subset with $r = 5$. Such equivalence validates that the sensor nodes selected using the proposed submodular set optimization framework are optimal. Furthermore, this demonstrates that only 5 sensor required to observe all the chemical species within the H_2O_2 network. This is also evident in Fig. 5 where it is shown that the estimation error approaches zero for the optimal solution when considering $r = 5$ for the H_2O_2 network. Note that the estimation error is related to the observability of the system. Such that, the estimation error is computed as $e = \|\mathbf{x} - \hat{\mathbf{x}}\|_2 / \|\mathbf{x}\|_2$, where \mathbf{x} is the true state and $\hat{\mathbf{x}}$ is the estimate obtained by solving a general nonlinear least squares state estimation problem for the observation horizon N .

For the H_2O_2 and GRI30 networks, we solve **P1** for the aforementioned sensor ratios and compute the estimation error. Notice that, for GRI30 network the estimation error decreases but does not reach an optimal error value due to a large number of non-interacting species. This indicates that additional sensors are required for better state estimation. We also note that utilizing a greedy approach yields an efficient and scalable solution to the observability-based SNS problem in nonlinear systems as compared with methods that rely on empirical data simulations—as with Empr-Gram framework. Solving **P1** for the H_2O_2 under sensor ratio 5/9 requires 0.414 s. The computational effort increases to about 24.797 s for GRI30 network when considering an equivalent sensor ratio. This shows that the proposed SNS framework is scalable for larger nonlinear networks. For brevity, we do not introduce

or solve the SNS framework based on the Empr-Gram, and therefore, we do not provide a comparison. However, based on the computational time provided in Tab. I, it is inferred that solving **P1** requires significantly more effort. The computational efficiency along with the optimality results provided by Fig. 4 and Fig. 5 validate the modularity of the proposed Var-Gram and its submodular observability measure log-det for SNS in nonlinear systems and thereby answers question Q3. On this note, we conclude this section.

VII. SUMMARY, LIMITATION AND FUTURE DIRECTIONS

This paper introduces a new observability Gramian for discrete-time nonlinear dynamical systems without inputs. The formulated nonlinear observability Gramian is based on a discrete-time variational nonlinear system representation. The Gramian is proved to be equivalent to the Empr-Gram and that it reduces to the observability Gramian when considering a linear system. Connections between the introduced observability notion and Lyapunov exponents are illustrated. We derive a spectral observability limitation result that arises from the proposed Var-Gram. To further showcase the validity of this approach, we demonstrate its applicability under the context of observability-based sensor node selection. The proposed observability notion, in its current form, is not devoid of limitations; further research is worthy of investigation. The method is developed for general nonlinear systems without considering control input. Nonlinear networks under control input will be considered in our future work. The equivalence between the Var-Gram and the Lyapunov exponents is demonstrated for the linear measurement model case. Thus, a generalized equivalence relation will be considered in future work. Furthermore, extension of this method for stochastic nonlinear systems with noisy measurements is important; such extension is demonstrated for the Empr-Gram [47].

APPENDIX A

RUNGE-KUTTA DISCRETE-TIME MODEL

The nonlinear mapping function $\tilde{f}(\cdot)$ is defined for the IRK method as

$$\tilde{f}(\mathbf{x}_0) := \frac{T}{4} (\mathbf{f}(\zeta_{1,k+1}) + 3\mathbf{f}(\zeta_{2,k+1})). \quad (27)$$

Vectors $\zeta_{1,k+1}, \zeta_{2,k+1} \in \mathbb{R}^{n_x}$ are auxiliary for computing \mathbf{x}_{k+1} provided that \mathbf{x}_k is given. As such, the IRK method results in the following implicit discrete-time state-space model

$$\begin{aligned} \zeta_{1,k+1} &= \mathbf{x}_k + \frac{T}{4} (\mathbf{f}(\zeta_{1,k+1}) - \mathbf{f}(\zeta_{2,k+1})), \\ \zeta_{2,k+1} &= \mathbf{x}_k + \frac{T}{12} (3\mathbf{f}(\zeta_{1,k+1}) + 5\mathbf{f}(\zeta_{2,k+1})), \\ \mathbf{x}_{k+1} &= \mathbf{x}_k + \frac{T}{4} (\mathbf{f}(\zeta_{1,k+1}) + 3\mathbf{f}(\zeta_{2,k+1})). \end{aligned} \quad (28)$$

The additional layer that includes calculating auxiliary vectors $\zeta_{1,k+1}$ and $\zeta_{2,k+1}$ allows an accurate and stable approach for the discretization of a broad class of nonlinear networks.

To evaluate the partial derivative of $\frac{\partial \tilde{f}(\mathbf{x}_k)}{\partial \mathbf{x}_0}$ for use in the discrete-time variational equations (10), we first need to compute the partial derivative $\frac{\partial \mathbf{x}_{k+1}}{\partial \mathbf{x}_k}$ which is involved numerically and can be written as follows

$$\begin{aligned} \frac{\partial \mathbf{x}_{k+1}}{\partial \mathbf{x}_k} &= \mathbf{I}_{n_x} + \frac{T}{4} \frac{\partial \mathbf{f}(\zeta_{1,k+1})}{\partial \zeta_{1,k+1}} \Big|_{\zeta_{1,k+1}^{(i)}} \frac{\partial \zeta_{1,k+1}}{\partial \mathbf{x}_k} \\ &+ \frac{3T}{4} \frac{\partial \mathbf{f}(\zeta_{2,k+1})}{\partial \zeta_{2,k+1}} \Big|_{\zeta_{2,k+1}^{(i)}} \times \frac{\partial \zeta_{2,k+1}}{\partial \mathbf{x}_k}. \end{aligned} \quad (29)$$

Notice that to determine $\frac{\partial \mathbf{x}_{k+1}}{\partial \mathbf{x}_k}$, we need to determine the partial derivatives $\frac{\partial \zeta_{1,k+1}}{\partial \mathbf{x}_k}$ and $\frac{\partial \zeta_{2,k+1}}{\partial \mathbf{x}_k}$. By differentiating (28) with respect to \mathbf{x}_k , we obtain

$$\underbrace{\begin{bmatrix} \frac{\partial \zeta_{1,k+1}}{\partial \mathbf{x}_k} \\ \frac{\partial \zeta_{2,k+1}}{\partial \mathbf{x}_k} \end{bmatrix}}_Q := \underbrace{\begin{bmatrix} \mathbf{I}_{n_x} \\ \mathbf{I}_{n_x} \end{bmatrix}}_{\mathbf{I}_{2n_x}} + \underbrace{\begin{bmatrix} \frac{T}{4} \frac{\partial \mathbf{f}(\zeta_{1,k+1})}{\partial \zeta_{1,k+1}} & -\frac{T}{4} \frac{\partial \mathbf{f}(\zeta_{2,k+1})}{\partial \zeta_{2,k+1}} \\ \frac{3T}{12} \frac{\partial \mathbf{f}(\zeta_{1,k+1})}{\partial \zeta_{1,k+1}} & \frac{5T}{12} \frac{\partial \mathbf{f}(\zeta_{2,k+1})}{\partial \zeta_{2,k+1}} \end{bmatrix}}_K \times \begin{bmatrix} \frac{\partial \zeta_{1,k+1}}{\partial \mathbf{x}_k} \\ \frac{\partial \zeta_{2,k+1}}{\partial \mathbf{x}_k} \end{bmatrix}. \quad (30)$$

Assuming that the matrix $[\mathbf{I}_{2n_x} - \mathbf{K}]$ is invertible (this is sufficient as a consequence of the implicit function theorem [31, Th. 3.3.1]), where $\mathbf{K} \in \mathbb{R}^{2n_x \times 2n_x}$, from the last expression, we have

$$\mathbf{Q} = [\mathbf{I}_{2n_x} - \mathbf{K}]^{-1} \mathbf{I}_{2n_x}. \quad (31)$$

After the matrix \mathbf{Q} has been computed, we can substitute its elements to calculate the partial derivatives (29).

Note that auxiliary vector $\zeta_{1,k+1}$ and $\zeta_{2,k+1}$ also depend on \mathbf{x}_0 . That is, to calculate the partial derivatives, we need to know the vectors $\zeta_{1,k+1}$ and $\zeta_{2,k+1}$. As such, these vectors can be obtained by simulating the system with initial condition equal to \mathbf{x}_0 . Based on the implicit nature of the auxiliary vectors, the vectors are embedded in the computation of $\frac{\partial \tilde{f}(\mathbf{x}_k)}{\partial \mathbf{x}_k}$; refer to (29)-(31). Then, the partial derivative $\frac{\partial \tilde{f}(\mathbf{x}_k)}{\partial \mathbf{x}_0}$ under the action of the chain rule can be written as

$$\frac{\partial \tilde{f}(\mathbf{x}_k)}{\partial \mathbf{x}_0} = \frac{\partial \tilde{f}(\mathbf{x}_k)}{\partial \mathbf{x}_k} \frac{\partial \mathbf{x}_k}{\partial \mathbf{x}_{k-1}} \frac{\partial \mathbf{x}_{k-1}}{\partial \mathbf{x}_{k-2}} \cdots \frac{\partial \mathbf{x}_1}{\partial \mathbf{x}_0}, \quad (32)$$

where by setting the time step k to j , the partial derivatives $\frac{\partial \mathbf{x}_j}{\partial \mathbf{x}_{j-1}}$ for all j can be computed from (29) as described above.

Note that the computation of $\frac{\partial \tilde{f}(\mathbf{x}_k)}{\partial \mathbf{x}_0}$ depends on the discretization method. Other methods follow similar derivations.

APPENDIX B

PROOF OF THEOREMS III.1, IV.1, AND V.1

For the proofs of theorems III.1 and IV.1, we consider a linear measurement model for the mapping function $\mathbf{h}(\mathbf{x}_k) = \mathbf{C}\mathbf{x}$. The reason for this choice of model is two-folds. (i) The linear mapping model simplifies the exposition of the proof and (ii) the linear measurement model is suitable for the analysis of sensors that measure only the states at the nodes where they are placed. We note that the choice of measurement model does not restrict the proofs; this follows as a consequence of Lemma IV.1. That being said, utilizing a linear measurement model proves theorems III.1 and IV.1 without the generality towards the scaling of matrix $\tilde{\mathbf{C}}(\mathbf{x}_k)$. The full proof is outside the scope of this paper. For additional considerations regarding generality toward nonlinear measurement mapping functions, the readers are referred to C.

Proof of Theorem III.1. The Empr-Gram (6) can be formulated in differential form by applying the central difference definition of a directional derivative on to the impulse response measurement vector $\Delta \mathbf{Y}_k^\varepsilon$ as (33), see [18], [28] for additional information.

$$\Delta \mathbf{Y}_k^\varepsilon = \left[2\varepsilon \frac{\partial \mathbf{y}_k}{\partial \mathbf{x}_0^1}, \dots, 2\varepsilon \frac{\partial \mathbf{y}_k}{\partial \mathbf{x}_0^{n_x}} \right]^\top, \quad (33)$$

where state vector $\mathbf{x}_0^i \in \mathcal{X}_0$ is denoted as $\mathbf{x}_0^i = \mathbf{x}_0 \pm \varepsilon \mathbf{e}_i \quad \forall i \in \{1, 2, \dots, n_x\}$, thus (33) is equivalent to $2\varepsilon \frac{\partial \mathbf{y}_k}{\partial \mathbf{x}_0}$. With that in mind, the Empr-Gram (6) can be written in the following form

$$\mathbf{W}_o^\partial(\mathbf{x}_0) := \sum_{k=0}^{N-1} \frac{\partial \mathbf{y}_k}{\partial \mathbf{x}_0}^\top \frac{\partial \mathbf{y}_k}{\partial \mathbf{x}_0}. \quad (34)$$

For simplicity of exposition, we consider a linear measurement model $\mathbf{h}(\mathbf{x}_k) = \mathbf{C}\mathbf{x}$. This does not restrict the proof since we are utilizing the same measurement model for both the Var-Gram and the Empr-Gram. It follows from (34) that for any time index k , we have $\frac{\partial \mathbf{y}_k}{\partial \mathbf{x}_0} \equiv \frac{\partial \mathbf{h}(\mathbf{x}_k)}{\partial \mathbf{x}_k} \frac{\partial \mathbf{x}_k}{\partial \mathbf{x}_0} = \mathbf{C} \frac{\partial \mathbf{x}_k}{\partial \mathbf{x}_0}$. In a similar approach considering the variational Gramian, we obtain $\Psi_0^k = \mathbf{C}\Phi_0^k = \mathbf{C}(\mathbf{I}_{n_x} + \frac{\partial \tilde{\mathbf{f}}(\mathbf{x}_k)}{\partial \mathbf{x}_k}) \frac{\partial \mathbf{x}_k}{\partial \mathbf{x}_0}$. Note that $\frac{\partial \mathbf{x}_{k+1}}{\partial \mathbf{x}_0} = (\frac{\partial \mathbf{x}_k}{\partial \mathbf{x}_0} + \frac{\partial \tilde{\mathbf{f}}(\mathbf{x}_k)}{\partial \mathbf{x}_0})$ is obtained by taking the partial derivative of (2a) about \mathbf{x}_0 and under the action of the chain rule, the partial derivative $\frac{\partial \mathbf{x}_k}{\partial \mathbf{x}_0}$ becomes a composition mapping similar to Ψ_0^k ; refer to Remark III.1. Hence, the two Gramians are equivalent and therefore the proof is complete. ■

Proof of Theorem IV.1. Let $\mathbf{h}(\mathbf{x}_k) = \mathbf{C}\mathbf{x}$. Then the observability matrix can be written as $\Psi = \left\{ \frac{\partial \mathbf{h}(\mathbf{x}_k)}{\partial \mathbf{x}_k} \Phi_0^k \right\}_{k=0}^{N-1} = \left\{ \mathbf{C}\Phi_0^k \right\}_{k=0}^{N-1}$. Now, from (14) for observation horizon N , and for $k \in \{0, 1, \dots, N-1\}$ it follows that

$$\begin{aligned} \mathbf{V}_o &= \sum_{k=0}^{N-1} \left[\mathbf{C} \prod_{1=0}^{i=k} \Phi_{i-1}^i \right]^\top \left[\mathbf{C} \prod_{1=0}^{i=k} \Phi_{i-1}^i \right], \\ &= \sum_{k=0}^{N-1} \left[\prod_{1=0}^{i=k} \Phi_{i-1}^i \right]^\top \mathbf{C}^\top \left[\mathbf{C} \prod_{1=0}^{i=k} \Phi_{i-1}^i \right], \\ &= \sum_{k=0}^{N-1} \prod_{1=0}^{i=k} \Phi_{i-1}^i \left[\mathbf{C} \prod_{1=0}^{i=k} \Phi_{i-1}^i \right]^\top, \end{aligned}$$

where $\mathbf{C}^\top \mathbf{C} = \mathbf{I}_{n_x} \in \mathbb{R}^{n_x \times n_x}$, considering a linear measurement model with sensors measuring all the states at each node. For case of measurement model that measures a subset of the states, \mathbf{I}_{n_x} is parameterized with the sensor parameterization vector γ . The above holds true as a result of inner product multiplication $\Psi^\top \Psi$ being equivalent to $\sum_{k=0}^{N-1} \Psi_0^k \Psi_0^k$. Following this, and based on the L2.2 property (Lemma IV.1), which holds true for Lyapunov exponents, we obtain the following by taking the log-det of \mathbf{V}_o .

$$\begin{aligned} \log\text{-det}(\mathbf{V}_o) &= \log\text{-det} \left(\sum_{k=1}^{N-1} \prod_{1=0}^{i=k} \Phi_{i-1}^i \right), \\ &= \log\text{-det} \left(\sum_{k=1}^{N-1} \|\Phi_0^k\|^2 \right), \\ &= \log\text{-det} \left(\Phi_0^{N-1 \top} \Phi_0^{N-1} \right), \\ &= \log \left(\prod_{i=1}^{n_x} \lambda_i \right) = \sum_{i=1}^{n_x} \log \lambda_i. \end{aligned}$$

On a similar note, taking the trace(λ_L) (19) for $k \rightarrow N \approx N-1$, and then computing the induced norm as $\|\Phi_0^k\| = \sqrt{\Phi_0^k \Phi_0^k}$, we obtain

$$\lim_{k \rightarrow N} \frac{1}{k} \log(\|\Phi_0^k\|) = \lim_{k \rightarrow N} \frac{1}{k} \log \left(\left(\Phi_0^k \Phi_0^k \right)^{1/2} \right),$$

$$= \frac{1}{2N} \lambda_L,$$

such that by evaluating the $\text{tr}(\frac{1}{2N} \lambda_L)$ we obtain $\frac{1}{2N} \sum_{i=1}^{n_x} \lambda_{L,i} = \sum_{i=1}^{n_x} \log \lambda_i$, this holds true given that λ_L is a diagonal matrix and with that the equivalence is proved. ■

Proof of Theorem V.1. For any $\mathcal{S} \subseteq \mathcal{V}$, observe that

$$\begin{aligned} \mathbf{V}_o(\mathcal{S}) &= \left[\left\{ \frac{\partial \mathbf{h}(\mathbf{x}_k)}{\partial \mathbf{x}_k} \Phi_0^k \right\}_{k=0}^{N-1} \right]^\top \left[\left\{ \frac{\partial \mathbf{h}(\mathbf{x}_k)}{\partial \mathbf{x}_k} \Phi_0^k \right\}_{k=0}^{N-1} \right], \\ &= \left[\mathbf{I} \otimes \Gamma \mathbf{C} \right] \left\{ \Phi_0^k \right\}_{k=0}^{N-1} \left[\mathbf{I} \otimes \Gamma \mathbf{C} \right] \left\{ \Phi_0^k \right\}_{k=0}^{N-1}, \\ &= \sum_{k=0}^{N-1} \left[\prod_{1=0}^{i=k} \Phi_{i-1}^i \right]^\top \left[\mathbf{C}^\top \Gamma^2 \mathbf{C} \right] \left[\prod_{1=0}^{i=k} \Phi_{i-1}^i \right], \end{aligned}$$

where $\Gamma^2 = \Gamma$, since it is a binary matrix. Now, denoting $\mathbf{c}_j \in \mathbb{R}^{1 \times n_x}$ as the j -th row of \mathbf{C} , then

$$\begin{aligned} \mathbf{V}_o(\mathcal{S}) &= \sum_{k=0}^{N-1} \left[\prod_{1=0}^{i=k} \Phi_{i-1}^i \right]^\top \left(\sum_{j=1}^{n_y} \gamma_j \mathbf{c}_j^\top \mathbf{c}_j \right) \left[\prod_{1=0}^{i=k} \Phi_{i-1}^i \right], \\ &= \sum_{j=1}^{n_y} \gamma_j \left(\sum_{k=0}^{N-1} \left[\prod_{1=0}^{i=k} \Phi_{i-1}^i \right]^\top \left[\mathbf{c}_j^\top \mathbf{c}_j \right] \left[\prod_{1=0}^{i=k} \Phi_{i-1}^i \right] \right), \\ &= \sum_{j \in \mathcal{S}} \left\{ \Phi_0^k \mathbf{c}_j^\top \mathbf{c}_j \Phi_0^k \right\}_{k=0}^{N-1} = \sum_{j \in \mathcal{S}} \mathbf{V}_o(j). \end{aligned}$$

Note that the notation $j \in \mathcal{S}$ corresponds to every activated sensor such that $\gamma_j = 1$. This shows that $\mathbf{V}_o(\mathcal{S})$ is a linear matrix function of γ_j satisfying modularity as $\mathbf{V}_o(\mathcal{S}) = \mathbf{V}_o(\emptyset) + \sum_{j \in \mathcal{S}} \mathbf{V}_o(j)$, (see Definition V.1). This concludes the proof. ■

APPENDIX C

NONLINEAR OUTPUT MAPPING FUNCTIONS

The following establishes how a generalized measurement function affects the derivation of certain equations within the proofs in this manuscript. The measurement equation can be written as

$$\Psi = \left\{ \frac{\partial \mathbf{h}(\mathbf{x}_k)}{\partial \mathbf{x}_k} \Phi_0^k \right\}_{k=0}^{N-1} = \left\{ \frac{\partial \mathbf{h}(\mathbf{x}_k)}{\partial \mathbf{x}_k} \prod_{1=0}^{i=k} \Phi_{i-1}^i \right\}_{k=0}^{N-1}, \quad (35)$$

thus the Var-Gram can be rewritten as,

$$\begin{aligned} \mathbf{V}_o(\mathbf{x}_0) &= \left[\frac{\partial \mathbf{h}(\mathbf{x}_1)}{\partial \mathbf{x}_1} \Phi_0^1, \frac{\partial \mathbf{h}(\mathbf{x}_2)}{\partial \mathbf{x}_2} \Phi_0^2, \dots, \frac{\partial \mathbf{h}(\mathbf{x}_{N-1})}{\partial \mathbf{x}_{N-1}} \Phi_0^{N-1} \right]^\top \\ &\quad \times \left[\frac{\partial \mathbf{h}(\mathbf{x}_1)}{\partial \mathbf{x}_1} \Phi_0^1, \frac{\partial \mathbf{h}(\mathbf{x}_2)}{\partial \mathbf{x}_2} \Phi_0^2, \dots, \frac{\partial \mathbf{h}(\mathbf{x}_{N-1})}{\partial \mathbf{x}_{N-1}} \Phi_0^{N-1} \right], \end{aligned} \quad (36)$$

while noting that the multiplication of any matrix-valued vector with its transpose is equivalent to its matrix dot-product, notice that we obtain a multiplication of two constant matrices at \mathbf{x}_i for all $i \in \{0, 1, \dots, N\}$ as follows

$$\begin{aligned} \Phi_{i-1}^i \left[\frac{\partial \mathbf{h}(\mathbf{x}_i)}{\partial \mathbf{x}_0} \right]^\top \frac{\partial \mathbf{h}(\mathbf{x}_i)}{\partial \mathbf{x}_0} \Phi_{i-1}^i &= \\ \left[\left(\mathbf{I}_{n_x} + \frac{\partial \tilde{\mathbf{f}}(\mathbf{x}_k)}{\partial \mathbf{x}_k} \right) \frac{\partial \mathbf{x}_k}{\partial \mathbf{x}_0} \right]^\top \mathbf{C}(\mathbf{x}_k) \mathbf{C}(\mathbf{x}_k) \left(\mathbf{I}_{n_x} + \frac{\partial \tilde{\mathbf{f}}(\mathbf{x}_k)}{\partial \mathbf{x}_k} \right) \frac{\partial \mathbf{x}_k}{\partial \mathbf{x}_0}, \end{aligned} \quad (37)$$

where $\Phi_0^k = \left(\mathbf{I}_{n_x} + \frac{\partial \tilde{\mathbf{f}}(\mathbf{x}_k)}{\partial \mathbf{x}_k} \right) \frac{\partial \mathbf{x}_k}{\partial \mathbf{x}_0}$ and $\mathbf{C}(\mathbf{x}_k) = \frac{\partial \mathbf{h}(\mathbf{x}_k)}{\partial \mathbf{x}_k}$. Thus, when constructing the Var-Gram, we obtain a multiplication of the differential of measurement mapping function (2b) with

respect to \mathbf{x}_k . The multiplication results in positive definite symmetric matrices $\tilde{\mathbf{C}}(\mathbf{x}_k) = \mathbf{C}(\mathbf{x}_k)^\top \mathbf{C}(\mathbf{x}_k)$, where $\mathbf{C}(\mathbf{x}_k)$ is a constant measurement matrix that measures at most all the states (under full sensor selection).

Based on Lemma IV.1, the matrix $\tilde{\mathbf{C}}$ results in scaling of the Lyapunov exponents while keeping the same indication of stability (negativeness/positiveness of the eigenvalues). This means that the Lyapunov exponents (eigenvalues) are scaled only; their indication of stability (negative or positive) is not altered. The derivations hold true for any regular positive matrix multiplying the state deformation matrices Φ_0^k .

REFERENCES

- [1] Y. Kawano and T. Ohtsuka, "Observability at an initial state for polynomial systems," *Automatica*, vol. 49, no. 5, pp. 1126–1136, 2013.
- [2] R. E. Kalman, "Mathematical Description of Linear Dynamical Systems," *Journal of the Society for Industrial and Applied Mathematics Series A Control*, vol. 1, no. 2, pp. 152–192, 1963.
- [3] R. Hermann and A. J. Krener, "Nonlinear Controllability and Observability," *IEEE Transactions on Automatic Control*, vol. 22, no. 5, pp. 728–740, 1977.
- [4] A. J. Whalen, S. N. Brennan, T. D. Sauer, and S. J. Schiff, "Observability and controllability of nonlinear networks: The role of symmetry," *Physical Review X*, vol. 5, no. 1, pp. 1–40, 2015.
- [5] A. J. Krener and K. Ide, "Measures of unobservability," *Proceedings of the IEEE Conference on Decision and Control*, pp. 6401–6406, 2009.
- [6] B. C. Moore, "Principal Component Analysis in Linear Systems: Controllability, Observability, and Model Reduction," *IEEE Transactions on Automatic Control*, vol. 26, no. 1, pp. 17–32, 1981.
- [7] S. Lall, J. E. Marsden, and S. Glavaški, "Empirical model reduction of controlled nonlinear systems," *IFAC Proceedings Volumes*, vol. 32, no. 2, pp. 2598–2603, 1999.
- [8] —, "A subspace approach to balanced truncation for model reduction of nonlinear control systems," *International Journal of Robust and Nonlinear Control*, vol. 12, no. 6, pp. 519–535, 2002.
- [9] L. Kunwoo, Y. Umezū, K. Konno, and K. Kashima, "Observability Gramian for Bayesian Inference in Nonlinear Systems with Its Industrial Application," *IEEE Control Systems Letters*, vol. 7, pp. 871–876, 2023.
- [10] A. Haber, F. Molnar, and A. E. Motter, "State Observation and Sensor Selection for Nonlinear Networks," *IEEE Transactions on Control of Network Systems*, vol. 5, no. 2, pp. 694–708, 2018.
- [11] M. H. Kazma, S. A. Nugroho, A. Haber, and A. F. Taha, "State-Robust Observability Measures for Sensor Selection in Nonlinear Dynamic Systems," *2023 62nd IEEE Conference on Decision and Control (CDC)*, no. Cdc, pp. 8418–8426, 2023.
- [12] Y. Y. Liu and A. L. Barabási, "Control principles of complex systems," *Reviews of Modern Physics*, vol. 88, no. 3, pp. 1–58, 2016.
- [13] Aleksandr Mikhailovich Lyapunov, "General Problem Of the Stability of Motion," 1892.
- [14] A. Czornik, A. Konyukh, I. Konyukh, M. Niezabitowski, and J. Orwat, "On Lyapunov and Upper Bohl Exponents of Diagonal Discrete Linear Time-Varying Systems," *IEEE Transactions on Automatic Control*, vol. 64, no. 12, pp. 5171–5174, 2019.
- [15] K. Krishna, S. L. Brunton, and Z. Song, "Finite Time Lyapunov Exponent Analysis of Model Predictive Control and Reinforcement Learning," *arXiv*, pp. 1–22, 2023.
- [16] L. Barreira, *Lyapunov Exponents*, 1998.
- [17] J. Cortés, A. Van Der Schaft, and P. E. Crouch, "Characterization of gradient control systems," *SIAM Journal on Control and Optimization*, vol. 44, no. 4, pp. 1192–1214, 2005.
- [18] Y. Kawano and J. M. Scherpen, "Empirical differential Gramians for nonlinear model reduction," *Automatica*, vol. 127, p. 109534, 2021.
- [19] M. Balcerzak, A. Dabrowski, B. Blazejczyk-Okolewska, and A. Stefanski, "Determining Lyapunov exponents of non-smooth systems: Perturbation vectors approach," *Mechanical Systems and Signal Processing*, vol. 141, p. 106734, 2020.
- [20] L. S. Young, "Mathematical theory of Lyapunov exponents," *Journal of Physics A: Mathematical and Theoretical*, vol. 46, no. 25, 2013.
- [21] A. Iserles, *A First Course in the numerical analysis of differential equations*, 2nd ed. Cambridge University Press, 2009.
- [22] K. E. Atkinson, W. Han, and D. Stewart, *Numerical Solution of Ordinary Differential Equations*. Wiley, jan 2009.
- [23] S. C. Shadden, F. Lekien, and J. E. Marsden, "Definition and properties of Lagrangian coherent structures from finite-time Lyapunov exponents in two-dimensional aperiodic flows," *Physica D: Nonlinear Phenomena*, vol. 212, no. 3–4, pp. 271–304, 2005.
- [24] D. K. Arrowsmith and C. M. Place, *Dynamical systems: differential equations, maps and chaotic behaviour*, first edit ed. Chapman and Hall, 1994.
- [25] S. Hanba, "Existence of an observation window of finite width for continuous-time autonomous nonlinear systems," *Automatica*, vol. 75, pp. 154–157, 2017.
- [26] —, "On the "Uniform" Observability of Discrete-Time Nonlinear Systems," *IEEE Transactions on Automatic Control*, vol. 54, no. 8, pp. 1925–1928, 2009.
- [27] S. Smale, "Mathematical problems for the next century," *The Mathematical intelligencer*, vol. 20, no. 2, pp. 7–15, 1998.
- [28] N. D. Powel and K. A. Morgansen, "Empirical observability Gramian rank condition for weak observability of nonlinear systems with control," *Proceedings of the IEEE Conference on Decision and Control*, vol. 54th IEEE, no. Cdc, pp. 6342–6348, 2015.
- [29] A. Mesbahi, J. Bu, and M. Mesbahi, "Nonlinear observability via Koopman Analysis: Characterizing the role of symmetry," *Automatica*, vol. 124, p. 109353, 2021.
- [30] D. Martini, D. Angeli, G. Innocenti, and A. Tesi, "Ruling Out Positive Lyapunov Exponents by Using the Jacobian's Second Additive Compound Matrix," *IEEE Control Systems Letters*, vol. 6, pp. 2924–2928, 2022.
- [31] S. G. Krantz and H. R. Parks, *The Implicit Function Theorem: History, Theory, and Applications*. Springer New York, 2013.
- [32] F. Pasqualetti, S. Zampieri, and F. Bullo, "Controllability metrics, limitations and algorithms for complex networks," *IEEE Transactions on Control of Network Systems*, vol. 1, no. 1, pp. 40–52, 2014.
- [33] T. H. Summers, F. L. Cortesi, and J. Lygeros, "On Submodularity and Controllability in Complex Dynamical Networks," *IEEE Transactions on Control of Network Systems*, vol. 3, no. 1, pp. 91–101, mar 2016.
- [34] A. Pikovsky and A. Politi, *Lyapunov Exponents: A Tool to Explore Complex Dynamics*. Cambridge University Press, 2017.
- [35] P. J. Nolan, M. Serra, and S. D. Ross, "Finite-time Lyapunov exponents in the instantaneous limit and material transport," *Nonlinear Dynamics*, vol. 100, no. 4, pp. 3825–3852, 2020.
- [36] M. Tranninger, R. Seeber, S. Zhuk, M. Steinberger, and M. Horn, "Detectability Analysis and Observer Design for Linear Time Varying Systems," *IEEE Control Systems Letters*, vol. 4, no. 2, pp. 331–336, 2020.
- [37] P. Manneville, "Characterization of Temporal Chaos," *Dissipative Structures and Weak Turbulence*, pp. 247–284, 1990.
- [38] J. Frank and S. Zhuk, "A detectability criterion and data assimilation for nonlinear differential equations," *Nonlinearity*, vol. 31, no. 11, pp. 5235–5257, 2018.
- [39] N. Barabanov, "Lyapunov exponent and joint spectral radius: Some known and new results," *Proceedings of the 44th IEEE Conference on Decision and Control, and the European Control Conference, CDC-ECC '05*, vol. 2005, no. 3, pp. 2332–2337, 2005.
- [40] G. Rota and W. Gilbert Strang, "A note on the joint spectral radius," *Indagationes Mathematicae (Proceedings)*, vol. 63, no. 638, pp. 379–381, 1960.
- [41] S. Joshi and S. Boyd, "Sensor selection via convex optimization," *IEEE Transactions on Signal Processing*, vol. 57, no. 2, pp. 451–462, 2009.
- [42] K. Manohar, J. N. Kutz, and S. L. Brunton, "Optimal Sensor and Actuator Selection Using Balanced Model Reduction," *IEEE Transactions on Automatic Control*, vol. 67, no. 4, pp. 2108–2115, 2022.
- [43] L. Lovász, *Submodular functions and convexity*. Berlin, Heidelberg: Springer Berlin Heidelberg, 1983, pp. 235–257.
- [44] L. Zhou and P. Tokekar, "Sensor Assignment Algorithms to Improve Observability while Tracking Targets," *IEEE Transactions on Robotics*, vol. 35, no. 5, pp. 1206–1219, 2019.
- [45] G. L. Nemhauser, L. A. Wolsey, and M. L. Fisher, "An analysis of approximations for maximizing submodular set functions-I," *Mathematical Programming*, vol. 14, no. 1, pp. 265–294, 1978.
- [46] N. N. Smirnov and V. F. Nikitin, "Modeling and simulation of hydrogen combustion in engines," *International Journal of Hydrogen Energy*, vol. 39, no. 2, pp. 1122–1136, 2014.
- [47] N. Powel and K. A. Morgansen, "Empirical Observability Gramian for Stochastic Observability of Nonlinear Systems," *arXiv*, jun 2020.